A NUMERICAL MODEL FOR THE CALCULATION OF FRETTING FATIGUE CRACK INITIATION FOR A SMOOTH LINE CONTACT

A. Lehtovaara[1,*], C. Lönnqvist[2], A. Mäntylä[2]
[1]Department of Mechanics and Design, Tampere University of Technology,
P.O. Box 589, 33101 Tampere, Finland
[2]Research & Development, Wärtsilä Finland Oy,
P.O. Box 244, 65101 Vaasa, Finland
*Corresponding author: tel: +358-3-311511, fax: +358-3-31152307, E-mail: arto.lehtovaara@tut.fi

ABSTRACT

A numerical model for the calculation of fretting fatigue crack initiation in smooth elastic contact is presented. The model is focused on cylinder-on-plane contact and it can be applied in partial and gross slip conditions by using a constant normal force, a reciprocating tangential force and a cyclic bulk stress. The model is based on explicit stress equations, the multi-axial Dang Van and Findley fatigue criteria and a statistical size factor concept. The model allows non-symmetric traction distribution caused by cyclic bulk stress and the calculation of relative tangential surface displacement. The results from the model correlate well with the corresponding FE-results. The model developed is fast.

Keywords: Fretting fatigue, cracking risk, Dang Van and Findley fatigue criterion, line contact

INTRODUCTION

Fretting may occur between any two contacting surfaces where short amplitude oscillatory movement is present. This causes fretting wear of the surfaces and fretting fatigue, which can lead to a rapid decrease in fatigue life. The appearance and severity of fretting fatigue is essentially dependent on the stress field on a contact (sub)surface caused by external bulk and contact loading. This stress field, affected by the oscillatory movement of the contacting surfaces, promotes crack nucleation. An extensive description of the fretting phenomenon and its associated contact mechanics is given in references [1- 3]. Fretting fatigue may cause hazardous and unexpected damage in machine components.

Fretting fatigue models are essential for researchers and designers to classify the importance of the design parameters involved in fretting fatigue and to obtain a detailed understanding of the fretting fatigue phenomenon. Design trend information is often as important as completely satisfactory prediction of the likelihood of crack initiation. A numerical model for the calculation of fretting fatigue crack initiation in smooth elastic sphere-on-plane contact and a related parameter study are presented in references [4, 5]. A model for the evaluation of the fretting fatigue in rough point contact has also been developed [6].

This study focuses on the development of the numerical model for the calculation of fretting fatigue crack initiation in smooth elastic cylinder-on-plane contact. The model is based on explicit stress equations, Dang Van and Findley multi-axial failure criteria and a statistical size factor concept. The results from the model are compared to corresponding FE results.

PROBLEM FORMULATION

A cylinder (body 1) and a plane (body 2) make contact with the forces and coordinates as shown in Fig. 1. The calculated stresses and cracking risk are related to body 2, where the external bulk stress in the x-direction also acts.

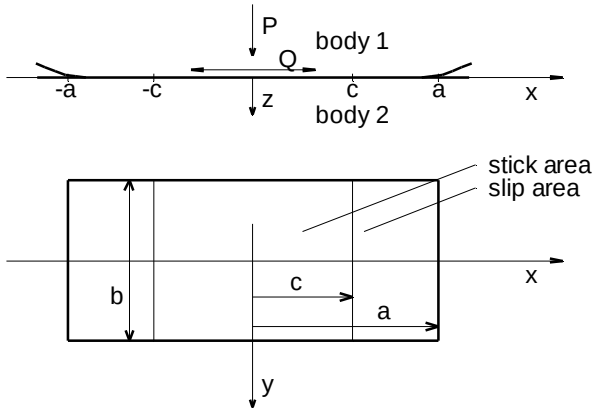

Figure 1. A schematic cylinder-on-plane contact.

Hertzian normal contact pressure distribution p is assumed in elastic cylinder-on-cylinder contact with smooth surfaces as follows:

$$p(x) = p_o\left(1-\frac{x^2}{a^2}\right)^{1/2} \tag{1}$$

where p_o is the maximum Hertzian pressure and a is the half width of the Hertzian line contact, which can be obtained as follows:

$$p_o = \frac{2P}{\pi ab} \tag{2}$$

$$a = \sqrt{\frac{4PR}{\pi E'b}} \tag{3}$$

In Eqs (2) and (3), P is the normal force, R is equivalent radius of curvature, E' is equivalent modulus of elasticity and b the length of the line contact. In the cylinder-on-plane case, R is simply the cylinder radius, but the formulation is also valid for the cylinder-on-cylinder contact cases using equivalent radius ($1/R = 1/R_1 + 1/R_2$). The equivalent modulus of elasticity is defined as: $1/E' = (1-\nu_1^2)/E_1 + (1-\nu_2^2)/E_2$ where E is the modulus of elasticity and ν is the Poisson ratio and subscripts 1 and 2 refer to bodies 1 and 2, respectively. The normal force P in the z-direction is assumed to be constant ($P = P_o$), while the tangential force Q in the x-direction is oscillating with an amplitude of $\pm Q_o$.

Once a tangential force is introduced, some sliding or at least partial slip between the contacting surfaces will occur. Assuming a constant friction coefficient μ over the slip zone, the tangential traction q caused by tangential motion inside the contact area is given according to [2, 7], by the following equations:

$$q(x) = \mu p_o\left(1-\frac{x^2}{a^2}\right)^{1/2}, \quad c \le x \le a \tag{4a}$$

$$q(x) = \mu p_o\left(1-\frac{x^2}{a^2}\right)^{1/2} - \mu p_o \frac{c}{a}\left(1-\frac{x^2}{c^2}\right)^{1/2}, \quad 0 \le x < c \tag{4b}$$

$$q(x) = 0, \qquad x > a \tag{4c}$$

where the half width of the stick zone c is:

$$c = a(1 - \frac{Q_o}{\mu P_o})^{1/2} \quad (5)$$

The partial slip condition in the contact will occur, when $Q < \mu P$. In this case, the surfaces in the central zone of the line contact will stick together whereas the outer zone will slip as shown in Fig. 1. If $Q = \mu P$, the tangential force is at its maximum and macroscopic sliding occurs between the surfaces. It is assumed that the effect of the tangential force on the normal pressure distribution and contact area is negligible.

The normal pressure and tangential traction at the contact surface cause stresses on and beneath the contact surface. The total macroscopic stress tensor $\Sigma_i(t)$ can be obtained from the sum of the stress tensors due to the constant normal force Σ_{iPo}, the cyclic external bulk stress $\Sigma_{iExt}(t)$, and the oscillating tangential force $\Sigma_{iQ}(t)$. It follows as:

$$\sum_i(t) = \sum_{iPo} + \sum_{iExt}(t) + \sum_{iQ}(t) \quad (6)$$

The macroscopic stress components due to normal and tangential forces at the general grid point i are obtained by introducing explicit equations for the stresses in a line contact surface according to [2, 3]. It is assumed that the half plane (body 2) is in a state of plane deformation. These equations are restricted to a macroscopic sliding case i.e. $Q = \mu P$, but they can also be applied to a partial slip case by superposing the separate tangential tractions of three different sliding cylinders with the same equivalent radius, but at different concentric regions with radii a, c and c'. Variable c' is the radius of the cyclic stick zone.

Fatigue criteria

Evaluation of fretting fatigue crack initiation is based on the multi-axial Dang Van and Findley fatigue criteria. Proportional loadings are assumed and the total macroscopic stress tensors $\Sigma_i(t_1)$ and $\Sigma_i(t_2)$, based on the two extreme loading conditions, are given as input values. Basically, if the cracking risk $d \geq 1$, failure will occur with a certain probability. This probability of failure can be determined by the probability theory for, preferably, both a log normal distributed stress and a log normal distributed strength.

The reference crack initiation risk d_{DVref} in body 2 with Dang Van criterion is given as [8]:

$$d_{DVref} = \max\left[\frac{\tau_a(t) + a_{href}\sigma_h(t)}{\tau_{afref}}\right] \quad (7)$$

The value of d_{DVref} obtained is the maximum value found during the load cycle. The shear fatigue limit τ_{afref} and the constant a_{href} are parameters of the material which can be determined with two uniaxial experimental fatigue tests. Hydrostatic stress σ_h is the bigger of the two hydrostatic stresses calculated from extreme loadings as:

$$\sigma_h(t) = trace(\sum_i(t))/3 \quad (8)$$

To obtain the shear stress amplitude $\tau_a(t)$, the microscopic shear stress tensor $\sigma_i(t)$ needs to be calculated as follows:

$$\sigma_i(t) = \sum_i(t) + dev(\rho_i^*) \quad (9)$$

The same magnitude of shear stress is obtained by using a macroscopic stress tensor from time 1 or time 2. ρ^* is the residual stress tensor which is assumed to be time independent and can be stated as;

$$\rho_i^* = -\frac{1}{2}\left(\sum_i(t_1) + \sum_i(t_2)\right) \quad (10)$$

The shear stress amplitude to be used in the Dang Van criterion can now be found by solving the principal stresses σ_I and σ_{III} ($\sigma_I > \sigma_{II} > \sigma_{III}$), resulting from Eq. (9):

$$\tau_a(t) = \frac{\sigma_I(t) - \sigma_{III}(t)}{2} \tag{11}$$

The critical plane is identified by the direction of the largest shear stress amplitude.

The reference crack initiation risk d_{Fref} in body 2 with the Findley criterion is given as [8]:

$$d_{Fref} = \max\left[\frac{\tau_a(t) + k_{Fref}\sigma_n(t)}{f_{Fref}}\right] \tag{12}$$

where τ_a is the shear stress amplitude and σ_n the normal stress on a shear plane. The shear fatigue limit f_{Fref} and the constant k_{Fref} are the material parameters. In the Findley criterion, the basic idea is to search the critical plane, where the damage $D = \tau_a(t) + k_{Fref} \cdot \sigma_n(t)$ on this plane, at any time during the load cycle, reaches its maximum value. The critical plane was searched by rotating the stress tensors $\Sigma_i(t_1)$ and $\Sigma_i(t_2)$ through all possible planes as follows:

$$\begin{aligned}\Sigma_i'(t_1) &= R_F^T \Sigma_i(t_1) R_F \\ \Sigma_i'(t_2) &= R_F^T \Sigma_i(t_2) R_F\end{aligned} \tag{13}$$

where R_F is the rotation matrix. The damage was studied on one face of the stress element and the rotation angles were varied within the range of 0 … 180 degrees. The calculation time required for rotation of the stress element was reduced using matrix methods. The shear stress amplitude τ_a at the face of stress element contains two shear stress components as follows:

$$\tau_a = \frac{1}{2}\sqrt{\Delta\tau_{axy}^2 + \Delta\tau_{axz}^2} \tag{14}$$

where $\Delta\tau_a$ is the shear stress difference between the two extreme stress states. The damage D can be stated as the bigger of the two values calculated from the extreme loadings. Finally, the maximum reference cracking risk can be obtained with Eq. (12), from the results for all the rotated planes. This also determines the critical plane.

Statistical size factor

Fretting contact includes extremely steep stress gradients both in depth and along the surface from the trailing edge. Because the fatigue limit is a random variable, it seems appropriate to use the theory of the weakest link to estimate the statistical size factor, which takes into account the difference between the effective stress area of the reference specimen used to test the Haigh diagram and the effective stress area of the contact zone. Moreover, this approach has the advantage of being generally applicable. The detailed background and description of the statistical size factor is given elsewhere [9]. Here, a short outline is given in a fretting line contact application.

The cracking risk d and the damage D over the fretting contact based on Dang Van and Findley criteria can already be calculated for a general grid point i. The standard normal variable λ_i and corresponding reliability $R_{d,i}$ for the different stress intervals are calculated with the following expressions:

$$\lambda_i = \frac{1}{s_r}\left(\frac{D_i}{D_{\max}} - 1\right) \tag{15}$$

$$R_{d,i} = \frac{1}{\sqrt{2\pi}} \cdot \int_{\lambda_i}^{\infty} e^{-\frac{x^2}{2}} dx \tag{16}$$

The maximum damage at the critical point is denoted by D_{max} and s_r is the expectation (sample) relative standard deviation (coefficient of variation). Eq. (15) and (16) are solved for every grid point i in the calculation domain. The effective stress area A_{eff} per single contact is given as:

$$A_{eff} = \sum \frac{\lg R_{d,i}}{\lg 0.5} \cdot A_i \tag{17}$$

In Eq. (17), A_i is the grid interval in the x-direction multiplied by the length of the line contact. The number of links n is the ratio of the effective stress area A_{ref} of the reference specimen used to test the Haigh diagram, to the effective stress area A_{eff} of the contact zone.

$$n = \frac{A_{ref}}{A_{eff}} \tag{18}$$

The expected contact fatigue limit has to be reduced to the probability of failure P_d given by the following equation to obtain the fatigue limit of the reference specimen:

$$P_d = 1 - \sqrt[n]{0.5} = 1 - R_d \tag{19}$$

The reliability R_d is given in Eq. (16), which allows for solving of the corresponding λ - value from the Eq. (19). Finally, using the log normal distribution, the statistical size factor K_{lsize} can be calculated as:

$$K_{lsize} = 10^{-\lambda s_{\lg}} \tag{20}$$

The logarithmic standard deviation $s_{\lg}$ can be evaluated directly from the staircase test of the fatigue limit by a maximum likelihood fit of the log normal density function to the test outcome. The actual fatigue limit at the contact is the statistical size factor K_{lsize} multiplied by the fatigue limit of the reference specimen used to test the Haigh diagram. It follows that the actual maximum cracking risk according to Dang Van d_{DV} and according to Findley d_F can be stated as;

$$d_{DV} = \frac{d_{DVref}}{K_{DVlsize}} \tag{21a}$$

$$d_F = \frac{d_{Fref}}{K_{Flsize}} \tag{21b}$$

$K_{DVlsize}$ refers to the statistical size factor related to Dang Van damage and K_{Flsize} to Findley damage.

Tangential displacement

The equations for the relative tangential surface displacement due to tangential load in cylinder-on-plane contact were also implemented in the model. The results are exact if the two bodies are elastically similar. They may also be used in contacts between elastically dissimilar bodies, but they are only approximate true under these conditions. The relative tangential surface displacement s_x caused by tangential sliding traction ($Q = \mu P$) is given by [2].

$$s_x(x) = \frac{\mu A P'}{\pi}\left[\left(\frac{x}{a}\right)^2 + C_o\right] \quad , \quad |x| \le a \tag{22a}$$

$$s_x(x) = \frac{\mu A P'}{\pi}\left[\ln|Xs| + \frac{1}{2Xs^2} + C_1\right], \quad |x| > a \tag{22b}$$

where

$$Xs = \left|\frac{x}{a}\right| + \sqrt{\left(\frac{x}{a}\right)^2 - 1} \tag{22c}$$

$$A = 2\left(\frac{1-\nu_1^2}{E_1} + \frac{1-\nu_2^2}{E_2}\right) \tag{22d}$$

$$P' = P / b \tag{22e}$$

It follows that:

$$s_x(x) = \mu p_o \left(\frac{\left(1-\nu_1^2\right)}{E_1} + \frac{\left(1-\nu_2^2\right)}{E_2} \right) \frac{x^2}{a} + C_{01}, \quad x \le a \tag{23a}$$

$$s_x(x) = \mu p_o \left(\frac{\left(1-\nu_1^2\right)}{E_1} + \frac{\left(1-\nu_2^2\right)}{E_2} \right) \cdot \ \ldots \ a\left[\ln\left|Xs\right| + \frac{1}{2Xs^2} + C_1 \right] \quad , \quad x > a \tag{23b}$$

The constants C_{01} and C_1 are arbitrary, but C_{01} should be chosen so that the displacement is continuous at the contact edge i.e. $x = \pm a$. In partial slip conditions, the relative tangential displacements are determined in a similar superposition manner to that in the case of stress components. The maximum slip is observed when x = ±*a*. Eqs (22a) and (22b) describes the total slip including both surfaces. The absolute displacement can not be determined. This inability to find the absolute displacement field is a characteristic of all 2D elasticity problems [2].

Non-symmetric traction distribution

It is known from the literature [2, 10] that in many experimental setups the tangential load is introduced by cyclic bulk stress as shown in Fig. 2.

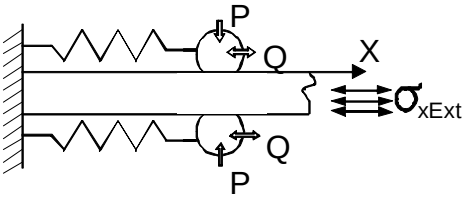

Figure 2. Common experimental setup for fretting tests.

In the setup shown in Fig. 2, the traction distribution is no longer axially symmetric due to the stick zone offset. The stick zone offset *e* for plane strain conditions can be expresses as [2].

$$e = \frac{\sigma_{aExt} a}{4\mu p_o} \tag{24}$$

where σ_{aExt} is the bulk stress amplitude in the x-direction. The traction distribution in the contact for the cyclic alternation of Q (= $\pm Q_a$) from reference [2] is:

$$q(x,e) = \mu p_o \left(1 - \frac{x^2}{a^2}\right)^{1/2}, \quad x_e > c, \quad x \le a \tag{25a}$$

$$q(x,e) = \mu p_o \left(1 - \frac{x^2}{a^2}\right)^{1/2} - \mu p_o \frac{c}{a}\left(1 - \frac{x_e^2}{c^2}\right)^{1/2}, \quad x_e \le c \tag{25b}$$

where

$$x_e = x - e \tag{25c}$$

Eq. (25) is organized in a similar way to Eq. (4). It reveals that in the case of two extreme loadings, the total tangential traction can be obtained by superposing the separate tangential tractions of two different sliding spheres with the same equivalent radius, but different concentric regions with radii *a* and *c*. The solution is valid if $e + c < a$, which means that the whole stick zone should be located inside the contact area.

FE-MODEL

The cylinder-on-plane situation described is shown in Fig. (2), and was also modelled with finite elements for comparison of the results. The FE model has been presented to International Symposium of Fretting Fatigue in Montreal [11]. A short summary is given here.

It was apparent from the results of the developed model that the element size must be very small with a size of less than one μm, to achieve realistic traction distribution and a corresponding stress field. Only a small part of the plane and cylinder using all the necessary boundary conditions could be modelled. The model and its boundary conditions in principle are shown in Fig. (3). The y-coordinate and σ_{bulk} in the FE model corresponds to the x-coordinate and σ_{aExt} in the developed fretting model.

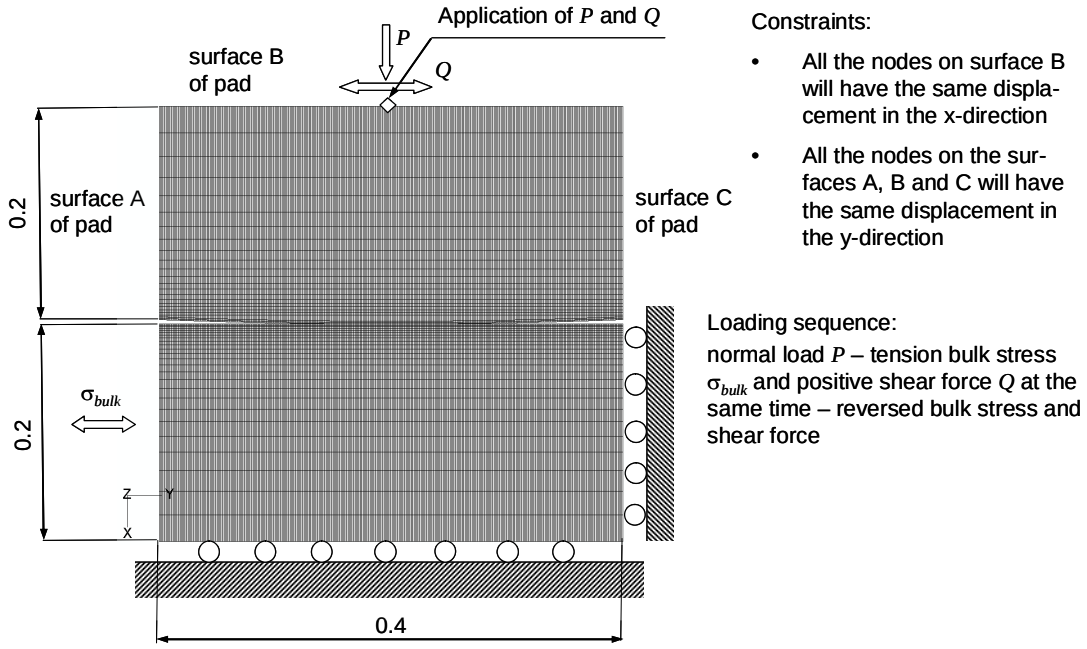

Figure 3. Nonlinear FE model for cylinder-on-plane contact (dimensions in mm) [11].

Although the explicit model is considered as a plain geometry, 8-node brick elements in one layer in the z-direction were used. A 3D model was used because the automated calculation of the effective stress area is not possible on 2D elements in the ABAQUS program used. Plain stress boundary conditions were used although it can be argued that a plain strain condition dominates towards the middle of the contact width. However, the Findley criterion calculates the same safety factor at the critical point regardless of whether a plain strain or a plain stress model has been used. This is because the Findley criterion orientates the critical plane in this particular situation in such a way that only the axial normal stress in the surface at that point will contribute to the damage.

Although, only such a small part of the system was modelled, the number of degrees of freedom rose to about 4 million when the element size was 0.25 μm. The convergence of the calculation was still checked with a model with a halved the element size to 0.125 μm, but with only the normal load and the tangential force. In addition convergence of the solution was analysed with three different element sizes (1.0 μm, 0.5 μm and 0.25 μm) by applying the normal force and the fully reversed tangential force. Finally, a penalty formulation with allowable elastic slip of 0.015 μm and an element size of 0.25 μm was used in the nonlinear contact analysis.

RESULTS AND DISCUSSION

The model stress field equations were initially tested successfully against the corresponding sliding line contact results given by Johnson [3]. Finally, the model was applied and compared to the cylinder-on-plane case, which was also modelled with finite elements and post-processed by Findley fatigue criterion and statistical size factor [11]. The calculation case includes also stick zone offset caused by the cyclic bulk stresses. Material related input values used in the Findley fatigue criteria for both the contacting bodies describe the properties of quenched and tempered steel 34CrNiMo6. They were derived from the experimental fatigue tests and are given as follows: Findley related material constant k_{Fref} = 0.29 and shear fatigue limit f_{Fref} = 380 MPa, The elasticity modulus of the material is 206 GPa and the Poisson ratio is 0.3. The effective stress area of the specimen used to test the Haigh diagram A_{ref} is 215 mm^2 and the sample relative standard deviation s_r is 0.065.

The calculated pressure distribution and traction distribution are shown in Fig. (4) and (5).

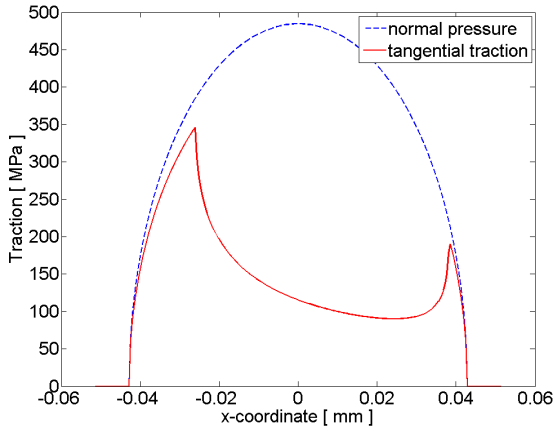

Figure 4. The pressure distribution and tangential traction distribution calculated with the developed model, P = 195.6 N, Q = 77.3 N, μ = 0.9, b = 6 mm, R = 5 mm, σ_{aExt} = ±248.7 MPa.

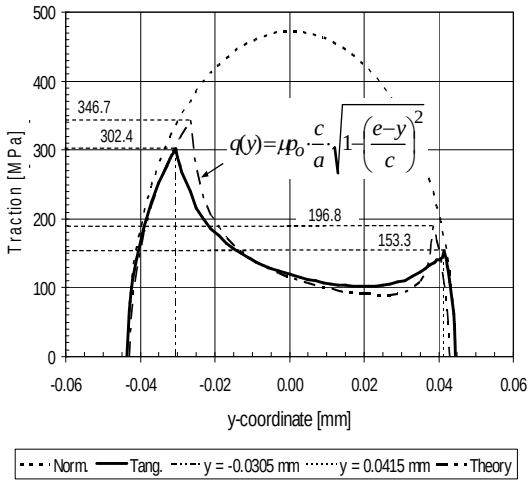

Figure 5. The corresponding distributions calculated with the FE model and compared to the theoretical tangential traction [11].

Figs. (4) and (5) show that the normal pressure distributions are very similar. According to the FE analysis the half width of the contact zone was 0.0435 mm which is fairly close to the theoretical value of 0.0428 mm calculated with the developed model. Correspondingly, finite element analysis gave a stick zone half width of c = 0.036 mm and a stick zone offset e = 0.0055 mm, which agree fairly well with the theoretical values (c = 0.032 mm, e = 0.0061 mm) obtained from the developed model. The tangential traction distribution calculated with the developed model has sharper peaks around the stick zone boundary than the FE-results, but otherwise the results are very much in the same order.

It has recently been found that this difference in ultimate peak shear traction is strongly related to the allowable elastic slip given in the FE-model. Decreasing the allowable elastic slip down to 1E-6 mm or using the Lagrange multiplier formulation strongly reduces this difference in peak shear traction as presented in reference [12].

However, the results calculated with an elastic slip of 0.015 μm are accurate enough for evaluation of the cracking risk behaviour in

the contact. The calculated Findley based cracking risks are shown in Figs. (6) and (7).

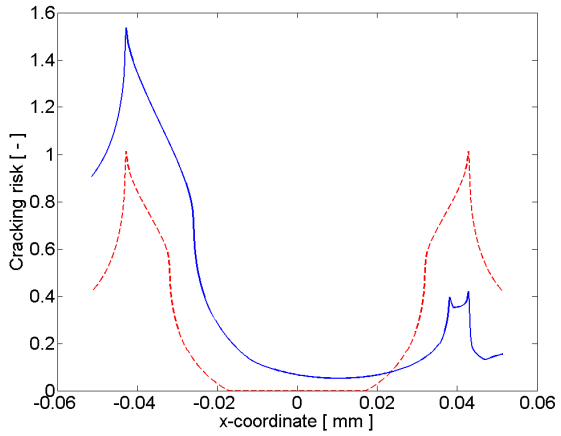

Figure 6. The Findley reference cracking risk d_{Fref}, with (solid line) and without (dashed line) external cyclic bulk stress calculated with the developed model, P = 195.6 N, Q = 77.3 N, μ = 0.9, b = 6 mm, R = 5 mm, σ_{aExt} = ±248.7 MPa.

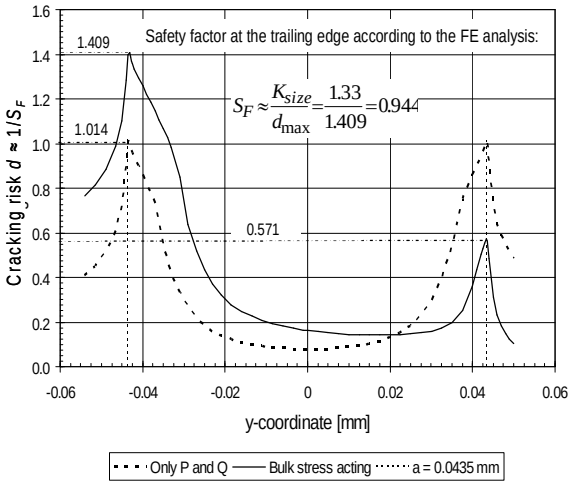

Figure 7. The corresponding Findley reference cracking risk d_{Fref}, with (solid line) and without (dashed line) external cyclic bulk stress calculated with the FE model [11].

It is shown in Figs. (6) and (7), that the general trends of the Findley based cracking risk curves are similar. The maximum model cracking risk peak is slightly sharper resulting in a value of 1.536, which is 9 % higher than the corresponding FE-result. This was expected due to the difference in tangential traction distribution. Without external bulk stress the correspondence of the cracking risk results are already very good. The statistical size factor was 1.32 calculated with the developed model and 1.33 calculated from the FE-results.

It can be concluded that the model results correlate well with the corresponding FE-results. The slight differences observed in peak values of tangential traction and cracking risk can mainly be explained by the magnitude of the allowable elastic slip in the FE model. The model developed is fast. The solution time for the results was less than 10 seconds using Intel Q9400 2.66 GHz personal computer. The potential for applying finite elements to fretting fatigue problems was also demonstrated. The advantage of finite elements is that they are not limited to any particular contact geometry.

CONCLUSIONS

A numerical model for the calculation of fretting fatigue crack initiation in smooth elastic contact is presented. The model is focused on cylinder-on-plane contact and it can be applied in partial and gross slip conditions. The model assumes proportional loading conditions with a constant normal force, a reciprocating tangential force and a cyclic bulk stress. The model is based on explicit stress equations, the multi-axial Dang Van and Findley fatigue criteria and a statistical size factor concept. The model allows non-symmetric traction distribution caused by cyclic bulk stress and the calculation of relative tangential displacement.

The model contact and cracking risk results correlate well with the corresponding FE-

results. The slight differences observed in peak values of tangential traction and cracking risk can mainly be explained by the magnitude of allowable elastic slip used in FE models. The model developed is fast. Moreover, the size of the calculation grid does not affect the accuracy of the executed stress state or reference cracking risk at the calculation points.

REFERENCES

[1]. Waterhouse, R.B. (Ed), Fretting Fatigue, Applied Science Publishers, Barking, 1981, p. 244.

[2] Hills, D.A., Novell, D., Mechanics of Fretting Fatigue, Dordrecht, Kluwer Academic Publishers, 1994, p. 236.

[3] Johnson, K.L., Contact Mechanics, Cambridge University Press, 1985, p. 452.

[4] Lehtovaara, A., Rabb, R., A numerical model for the calculation of fretting fatigue crack initiation for a smooth spherical contact, Finnish J. of Tribology, 25 (2006) 23-30.

[5] Lehtovaara, A., Rabb, R., Fretting fatigue crack initiation for a smooth spherical contact – a parameter study, Finnish J. of Tribology, 25 (2006) 31-40.

[6] Lehtovaara, A., Rabb, R., A numerical model for the evaluation of fretting fatigue crack initiation in rough point contact, Wear 264 (2008) 750-756.

[7] Mindlin, R. D., Compliance of Elastic Bodies in Contact, J Appl Mech 16 (1949) 259-268.

[8] D.F. Socie, G.B. Marquis, Multiaxial Fatigue, Warrendale, SAE Publications Group, 2000, p. 484.

[9] Rabb, R., Interpretation and Evaluation of the Statistical Size Effect, Proc. of 23rd CIMAC World Congress on Combustion and Engine Technology, May 2001, pp.1125-1138.

[10] Cadario, A., Alfredsson, B., Fretting Fatigue Crack Growth for a Spherical Indenter with Constant and Cyclic Bulk Load, Eng. Fracture Mech. 72 (2005) 1664-1690.

[11] Rabb, R., Hautala, P. and Lehtovaara, A., Fretting Fatigue in Medium-Speed Diesel Engines, Presented in Int. Symp. for Fretting Fatigue (ISFF5), April 24-26, 2007, Montreal, Canada

[12] Mäntylä, A., Lönnqvist, C., Fretting Simulation for Crackshaft-Counterweight Contact, SIMULIA Customer Conference, May 2009, London, England.